BULLETIN OF THE POLISH ACADEMY OF SCIENCES
TECHNICAL SCIENCES, Vol. 69(3), 2021, Article number: e137064
DOI: 10.24425/bpasts.2021.137064

Research on hybrid modeling and predictive energy management for power split hybrid electric vehicle

Shaohua WANG[1], Sheng ZHANG[1], Dehua SHI[1,2,3]*, Xiaoqiang SUN[1], and Tao YANG[3]

[1] Automotive Engineering Research Institute, Jiangsu University, Zhenjiang 212013, China
[2] Vehicle Measurement, Control and Safety Key Laboratory of Sichuan Province, Xihua University, Chengdu 610039, China
[3] Jiangsu Chunlan Clean Energy Research Institute Co., Ltd., Taizhou 225300, China

Abstract. Due to the coexistence of continuity and discreteness, energy management of a multi-mode power split hybrid electric vehicle (HEV) can be considered a typical hybrid system. Therefore, the hybrid system theory is applied to investigate the optimum energy distribution strategy of a power split multi-mode HEV. In order to obtain a unified description of the continuous/discrete dynamics, including both the steady power distribution process and mode switching behaviors, mixed logical dynamical (MLD) modeling is adopted to build the control-oriented model. Moreover, linear piecewise affine (PWA) technology is applied to deal with nonlinear characteristics in MLD modeling. The MLD model is finally obtained through a high level modeling language, i.e. HYSDEL. Based on the MLD model, hybrid model predictive control (HMPC) strategy is proposed, where a mixed integer quadratic programming (MIQP) problem is constructed for optimum power distribution. Simulation studies under different driving cycles demonstrate that the proposed control strategy can have a superior control effect as compared with the rule-based control strategy.

Key words: power split HEV; energy management; mixed logical dynamical model; piecewise affine; model predictive control.

1. Introduction

HEVs have two or more power sources and can recover some kinetic energy when braking. They have acquired a certain share in today's automobile market for their excellent fuel economy. Among different HEV types, the power split ones are most attractive. Usually, the power split HEV adopts planetary gear sets as its power coupling device, because the multi freedom degrees of the planetary gear sets make it possible for the engine to decouple the torque and speed from those at wheels. As a result, more efficiency operation of the engine is achieved [1–3]. Nowadays, various configurations with power split device have been proposed, such as THS, THS-II, GM-2mode, etc. [4–6] In some power coupling devices, additional brakes and clutches are often applied to achieve higher transmission efficiency and more operation modes [7, 8].

Once the configuration of the power coupling device is determined, an efficient energy management strategy is necessary to regulate power distribution among different power components. Two main kinds of energy management strategies can be observed [9]. One is the rule based strategy, which has been widely used in mass-produced HEVs, such as the Prius, Volt and Fusion. The rule based strategy shows good robustness and easy implementation. However, the control effect may be quite far from the optimal solution. For the HEV, in order to maintain charging sustainability, the optimum solution is exact battery balance, which means equal initial and final battery SOC (state of charge). Lowest engine fuel consumption should also be controlled. The optimal solution can be derived by means of global optimal algorithms. Meanwhile, the decision rules rely strongly on engineering practice and expert experience. The other kind of strategy is the optimization based strategy and optimal energy management is regarded as a type of a constrained optimization problem. Control constrains include the driving requirements and the physical operation limits of different power components, such as the torque and speed of electric machines along with variation of the battery SOC due to the battery charging sustaining, while the optimization object is usually the fuel economy and exhaust emission. Optimization based strategy can obtain optimal or near-optimal results by solving constrained optimal problems. For example, the dynamic programming (DP) algorithm, a type of global optimization strategy based on the Bellman's principle, is usually integrated into the control of HEVs [10]. Although the control effect is theoretically optimal, there is little chance for this strategy to be put in practice because of the heavy computational burden and the demand for prior knowledge of the cycle. Instead, the result of the global optimization strategy is usually used as the benchmark to evaluate the performance of other strategies. For online application, equivalent consumption minimization strategy (ECMS) is designed, which is a type of instantaneous optimization strategy [11, 12]. ECMS shows good real-time capability. However, the solution is near-optimal. Meanwhile, the equivalent factor between electric consumption and fuel consumption is difficult to obtain.

*e-mail: dhshi@ujs.edu.cn

Manuscript submitted 2019-11-06, revised 2021-02-27, initially accepted for publication 2021-03-26, published in June 2021

To overcome the shortcomings of the global optimization strategy and instantaneous optimization strategy, model predictive control (MPC), which is capable of dealing with multi-inputs and multi-outputs problems in the finite time horizon [13], is proposed to optimize the power split over a receding horizon by incorporating the future running condition into the optimization. An accurate prediction is quite significant for MPC strategy and the development of global positioning and communications technology make it possible to accurately predict the future running condition. At the same time, the control-oriented model that the MPC strategy is based on exerts strong influence over the solutions. Of the two different MPC strategies, one is a standard MPC method for linear systems and the other is based on Hamilton-Jacobi-Bellman equation. They are introduced and demonstrate good control effects in improving vehicle fuel economy [14].

As for power split HEVs integrated with multiple clutches and/or brakes, they have abundant operation modes with the engagement/disengagement states of the clutches and/or brakes possible, leading to different power distribution processes. The energy management process shows the coexistence of continuity and discreteness. Specifically, in each operation mode of the multi-mode power split HEV, the system state variables, such as the fuel consumption rate and battery SOC, evolve according to the system dynamic equations constrained by their own physical properties. This is a typical continuous dynamic process. While the state variables evolve to break through the predefined threshold, HEV operation mode is switched. The discreteness of the energy management process lies in the mode switching and on/off states of different components. The mode switching and continuous state evolution interact [15]. Therefore, it is hard to reflect on the dynamic nature of HEV by simplifying the model just in terms of continuous or discrete states. By reviewing the existent studies, it can be concluded that almost all the energy management strategies of the HEVs are designed by viewing the system to be continuous for the purpose of reducing modeling difficulty, for example, by rendering the system linear through Taylor expansion. As a result, the system's operation nature cannot be accurately described.

Aiming at the hybrid dynamic nature when the HEV operation modes switch frequently, it is vital to build an accurate power management model that can feature the discrete event switch under the whole driving cycle. Therefore, hybrid system theory is innovatively introduced in this paper to describe the interactions between system continuity and discreteness. Based on the hybrid theory, operation modes of the HEV are described by binary variables and the power distribution process under different modes can be unified and obtained. The unified model includes both continuous parts and discrete parts of the system. Hybrid system theory has developed fast in recent years, and it has been widely used in practical engineering [16–18]. The established hybrid model is further used for optimal energy management.

Specifically, the rest of the paper is organized as follows. In Section 2, configuration of the HEV is introduced and the hybrid characteristics are analyzed. Based on hybrid system theory and linear piecewise affine technology, the MLD model is constructed in Section 3. Section 4 establishes the HMPC, followed by the simulation study in Section 5. Finally, Section 6 draws the conclusions.

2. System description

2.1. Configuration of the HEV. The schematic diagram of the power split HEV is shown in Fig. 1. The power coupling device consists of two planetary gear sets, P1 and P2. Carrier C1 is connected to ring gear R2, and ring gear R1 is connected to carrier C2. The engines, MG1 and MG2, are connected to C1, S1 and S2, respectively. Ring gear R2 acts as the output shaft and transmits the power to the wheel through the final drive. MG1 and MG2 can both work as an electric motor or electric generator. Additionally, two brakes, B1 and B2, are set between the engine and C1, MG1 and S1, respectively.

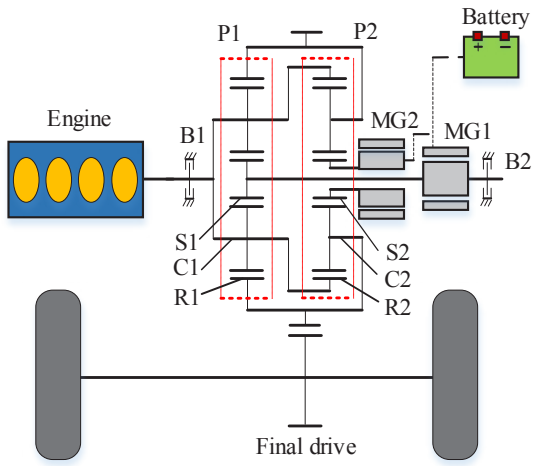

Fig. 1. Structure of HEV. P1/2 – planetary gear set 1/2; S1/2 – sun gear 1/2; C1/2 – carrier 1/2; R1/2 – ring gear 1/2; MG1/2 – electric machine 1/2; B1/2 – brake 1/2

2.2. Analysis of hybrid characteristics. Feasible operation modes of the HEV are listed in Table 1. It also depicts the operating states of the brakes, engine, MG1 and MG2 in each mode, where "E" represents "engaged" and "D" represents "disengaged". It can be seen that six vehicle operation modes are divided according to different combinations of power sources and

Table 1
Operation modes of HEV

Mode	Engine	MG1	MG2	B1	B2
Pure electric driving	off	off	on	E	D
Engine driving	on	off	off	D	E
Hybrid driving	on	on	on	D	D
Compound braking	off	off	on	E	D
Charging standstill	on	on	off	D	D
Stop	off	off	off	E	E

brakes. Torque and speed relations within the system vary with the operation modes and can be derived according to lever analogy under the assumption that all shafts are rigid and inertias of the gears in planetary gear sets are ignored [14, 19].

In the pure electric driving mode that only MG2 works, the torque and speed relations are shown as follows:

$$\begin{cases} T_{\mathrm{e}} = 0, \\ T_{\mathrm{MG1}} = 0, \\ T_{\mathrm{MG2}} = (1+k_2)^{-1} T_{req}, \\ \omega_{\mathrm{e}} = 0, \\ \omega_{\mathrm{MG1}} = -k_1 \omega_{out}, \\ \omega_{\mathrm{MG2}} = (1+k_2)\omega_{out}. \end{cases} \tag{1}$$

In engine driving mode, the engine drives the vehicle alone and the steady relation is:

$$\begin{cases} T_{\mathrm{e}} = (1+k_1)k_1^{-1} T_{req}, \\ T_{\mathrm{MG1}} = 0, \\ T_{\mathrm{MG2}} = 0, \\ \omega_{\mathrm{e}} = k_1(1+k_1)^{-1}\omega_{out}, \\ \omega_{\mathrm{MG1}} = 0, \\ \omega_{\mathrm{MG2}} = (1+k_1+k_2)(1+k_1)^{-1}\omega_{out}. \end{cases} \tag{2}$$

In hybrid driving mode, all power sources participate in the action. The steady relation is:

$$\begin{cases} T_{\mathrm{MG1}} = [k_2 T_{req} - (1+k_2)T_{\mathrm{e}}] \cdot (1+k_1+k_2)^{-1}, \\ T_{\mathrm{MG2}} = [(1+k_1)T_{req} - k_1 T_{\mathrm{e}}] \cdot (1+k_1+k_2)^{-1}, \\ \omega_{\mathrm{MG1}} = (1+k_1)\omega_{\mathrm{e}} - k_1 \omega_{out}, \\ \omega_{\mathrm{MG2}} = (1+k_2)\omega_{out} - k_2 \omega_{\mathrm{e}}. \end{cases} \tag{3}$$

In compound braking mode, braking force comes from MG2 and the mechanical brake system. MG2 is used as much as possible to recuperate the energy, and the torque and speed relations in this process can be obtained as:

$$\begin{cases} T_{\mathrm{e}} = 0, \\ T_{\mathrm{MG1}} = 0, \\ T_{\mathrm{MG2}} = \max\left\{T_{\mathrm{MG2\_max}}, (1+k_1)^{-1} T_{req}\right\}, \\ \omega_{\mathrm{e}} = 0, \\ \omega_{\mathrm{MG1}} = -k_1 \omega_{out}, \\ \omega_{\mathrm{MG2}} = (1+k_2)\omega_{out}. \end{cases} \tag{4}$$

In charging standstill mode, the engine drives MG1 to generate electricity. Mechanical braking system provides braking force to keep the vehicle still, and in this mode, we have:

$$\begin{cases} T_{\mathrm{MG1}} = -(1+k_1)^{-1} T_{\mathrm{e}}, \\ T_{\mathrm{MG2}} = 0, \\ \omega_{\mathrm{MG1}} = (1+k_1)\omega_{\mathrm{e}}, \\ \omega_{\mathrm{MG2}} = -k_2 \omega_{\mathrm{e}}. \end{cases} \tag{5}$$

In stop mode, the torque and speed of different components are as follows:

$$\begin{cases} T_{\mathrm{e}} = T_{\mathrm{MG1}} = T_{\mathrm{MG2}} = T_{req} = 0, m, \\ \omega_{\mathrm{e}} = \omega_{\mathrm{MG1}} = \omega_{\mathrm{MG2}} = \omega_{out} = 0. \end{cases} \tag{6}$$

In (1)–(4), T_{e} is the engine torque; T_{MG1} is MG1 torque; T_{MG2} is MG2 torque; $T_{\mathrm{MG2\_max}}$ is the maximum values of T_{MG2}; T_{req} is the required torque at the output side of the coupling device; ω_{e} is engine speed; ω_{MG1} is MG1 speed; ω_{MG2} is MG2 speed; ω_{out} is output speed of the coupling device; k_1 and k_2 are characteristic parameters of planetary gear sets.

In order to ensure good fuel economy, the proposed power coupling device switches among different modes and the operation of different power sources, such as the engine and electric machines, vary from the modes. The mode switch is represented by event-driven rather than by time-driven dynamics [20]. The driven events rely on the continuous time-related state variables, such as the battery SOC, vehicle speed etc. Therefore, the mode switch demonstrates typical discrete dynamics. On the other hand, in each operation mode of the power coupling device, the time-related variables are decided by the corresponding evolution law constrained by the physical properties in each mode. The evolution of the time-related state variables is a typical continuous dynamic process. The relations between the discrete modes and the continuous state evolution are shown in Fig. 2. Therefore, the energy management process of the power split HEV involves interaction of the discrete mode switch and continuous state evolution. This can be viewed as a hybrid system [21].

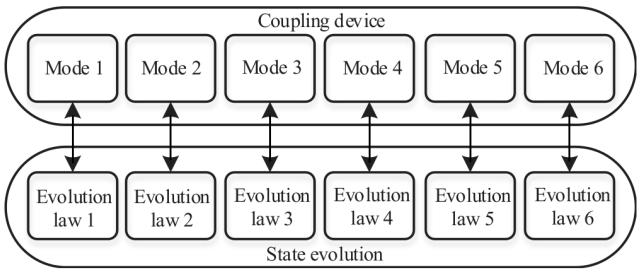

Fig. 2. Hybrid phenomenon

3. MLD modeling

Several modeling frameworks have been developed to describe the hybrid system, among which the mixed logical dynamical (MLD) model allows for specifying the evolution of binary variables through propositional logic and finite automata and the evolution of continuous variables through linear dynamic equations, as well as the mutual interaction between binary and continuous variables [22]. It is convenient to be used as a control-oriented model in the optimization problem. The MLD model has the form as presented below:

$$\begin{cases} \boldsymbol{x}(t+1) = \boldsymbol{A}\,\boldsymbol{x}(t) + \boldsymbol{B}_1 \boldsymbol{u}(t) + \boldsymbol{B}_2 \boldsymbol{\delta}(t) + \boldsymbol{B}_3 z(t), \\ \boldsymbol{y}(t) = \boldsymbol{C}\,\boldsymbol{x}(t) + \boldsymbol{D}_1 \boldsymbol{u}(t) + \boldsymbol{D}_2 \boldsymbol{\delta}(t) + \boldsymbol{D}_3 z(t), \\ \boldsymbol{E}_2 \boldsymbol{\delta}(t) + \boldsymbol{E}_3 z(t) \le \boldsymbol{E}_1 \boldsymbol{u}(t) + \boldsymbol{E}_4 \boldsymbol{x}(t) + \boldsymbol{E}_5, \end{cases} \tag{7}$$

where x is the state variable, which has the form of $x = [x_c, x_d]^T$, containing both continuous state variables $x_c \in R^{nc}$ and binary state variables $x_d \in R^{nd}$. Similar definitions are also applied to control variable u and output variable y. $\delta \in [0, 1]^{rd}$ and $z \in R^{rc}$ are the auxiliary binary variable and auxiliary continuous variable introduced for the requirement of modeling. $\boldsymbol{A}$, $\boldsymbol{B}_{1-3}$, $\boldsymbol{C}$, $\boldsymbol{D}_{1-3}$, $\boldsymbol{E}_{1-5}$ are constant matrices of suitable dimensions.

The framework of the MLD model for the energy management system of the multi-mode HEV is shown in Fig. 3. From aforementioned analysis, it can be found that the discrete characteristics of the power coupling device lead to the hybrid characteristics of the HEV energy management system. Since the objective of the optimal power distribution is to determine the engine operating point while meeting the requirement of the driving condition, the required torque T_{req}, output speed ω_{out}, engine torque T_e and engine speed ω_e are chosen to be the inputs of the MLD model. Meanwhile, battery SOC is chosen as the state variable and it evolves over time. The fuel consumption rate is the output variable. The states of the power coupling devices are discrete variables which can be determined by the input set.

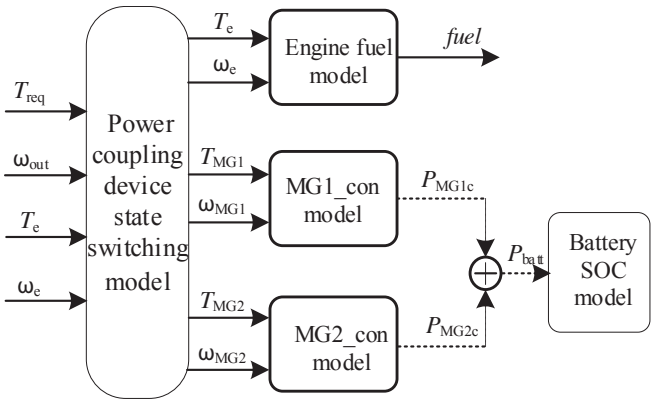

Fig. 3. Framework of the MLD model for power split HEV

In order to apply linear hybrid modeling and optimization techniques, nonlinear relations between the inputs and outputs are approximated by means of piecewise affine (PWA) technology [23, 24]. There are two types of nonlinear models in the system. One type of the nonlinear models are two-dimensional, including torque limit models of the engine, MG1, MG2 and the battery SOC model. The other type of models demonstrate three-dimensional characteristics, for example, the engine fuel model and the input power models of MG1 and MG2.

For two-dimensional models, the multi parameter optimization method is applied. 3, 5, 7 and 2 straight lines are used for the linearization of the torque limit models of the engine, MG1, MG2 and the battery SOC model, respectively, as follows:

$$\begin{cases} T_{ex}^i = [\omega_e \;\; 1]\theta_{ex}^i; & \omega_e \in A_e^i \quad i = 1,2,3, \\ T_{gx}^i = [\omega_{MG1} \;\; 1]\theta_{gx}^i; & \omega_{MG1} \in A_g^i \quad i = 1,2,\ldots,5, \\ T_{mx}^i = [\omega_{MG2} \;\; 1]\theta_{mx}^i; & \omega_{MG2} \in A_m^i \quad i = 1,2,\ldots,7, \\ C_{batt}^i = [P_{batt} \;\; 1]\theta_{bx}^i; & P_{batt} \in A_{batt}^i \quad i = 1,2, \end{cases} \tag{8}$$

where T_{ex}, T_{gx} and T_{mx} are linearized torque limits of engine, MG1 and MG2; C_{batt} is the linearized SOC change rate; θ is the corresponding line parameter vector; A_e, A_g, A_m and A_{batt} are the corresponding affine regions of different components; i is the quantity of straight lines. Linearization of different two-dimensional models is shown in Fig. 4.

For the three-dimensional models, the clustering-based method is applied [24]. 4, 14 and 18 planes are used for lin-

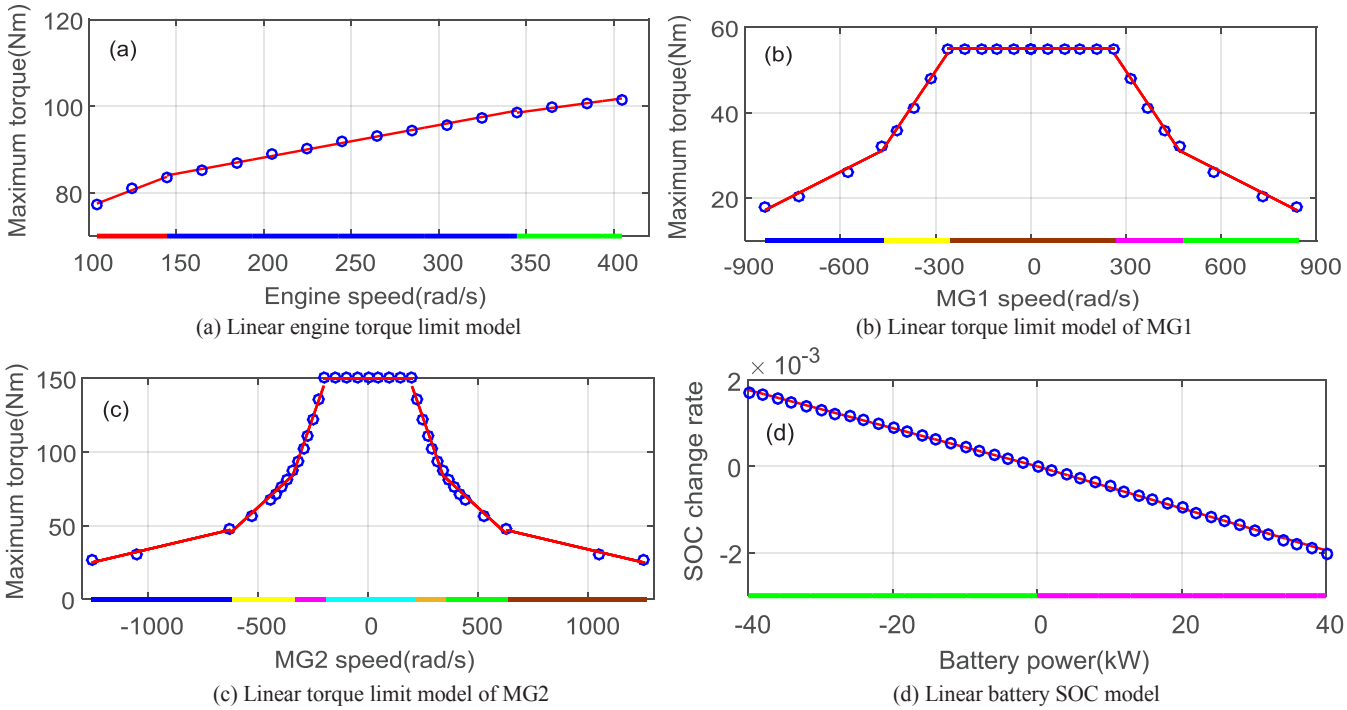

(a) Linear engine torque limit model

(b) Linear torque limit model of MG1

(c) Linear torque limit model of MG2

(d) Linear battery SOC model

Fig. 4. Linearization of two-dimensional models

earization of the engine fuel model and input power models of MG1 and MG2, respectively.

$$\begin{cases} f_{\mathrm{e}}^{i} = [T_{\mathrm{e}} \;\; \omega_{\mathrm{e}} \;\; 1]\theta_{ef}^{i}; \quad (T_{\mathrm{e}}, \omega_{\mathrm{e}}) \in \Omega_{ef}^{i}, \quad i = 1,2,3,4, \\ P_{\mathrm{gp}}^{i} = [T_{\mathrm{MG1}} \;\; \omega_{\mathrm{MG1}} \;\; 1]\theta_{\mathrm{gp}}^{i}; \quad (T_{\mathrm{MG1}}, \omega_{\mathrm{MG1}}) \in \Omega_{\mathrm{gp}}^{i}, \\ \qquad\qquad\qquad\qquad\qquad\qquad i = 1,2,\ldots,14, \\ P_{\mathrm{mp}}^{i} = [T_{\mathrm{MG1}} \;\; \omega_{\mathrm{MG2}} \;\; 1]\theta_{\mathrm{mp}}^{i}; \quad (T_{\mathrm{MG2}}, \omega_{\mathrm{MG2}}) \in \Omega_{\mathrm{mp}}^{i}, \\ \qquad\qquad\qquad\qquad\qquad\qquad i = 1,2,\ldots,18, \end{cases} \tag{9}$$

where f_{e}, P_{gp} and P_{mp} are linearized powers of the engine, MG1 and MG2, respectively; C_{batt} is the linearized SOC change rate; θ_{ef}, θ_{gp} and θ_{mp} are corresponding plane parameter vectors; Ω_{ef}, Ω_{gp} and Ω_{mp} are corresponding affine regions; i is the quantity of straight lines. Linearization of different models is shown in Fig. 5.

In order to accurately express the constraints and evolution mechanisms for different variables in the MLD model using HYSDEL, auxiliary variables are introduced [25]. Auxiliary continuous variables ω_{g} and ω_{m} are defined according to the system inputs to represent the speed of MG1 and motor MG2, as follows:

$$\begin{cases} \omega_{\mathrm{g}} = (1+k_1)\omega_{\mathrm{e}} - k_1\omega_{\mathrm{out}}, \\ \omega_{\mathrm{m}} = (1+k_2)\omega_{\mathrm{out}} - k_2\omega_{\mathrm{e}}. \end{cases} \tag{10}$$

Aiming at the external characteristic curves of engines and motors, auxiliary discrete variables δ_{ex}^{i}, δ_{gx}^{i} and δ_{mx}^{i} are defined respectively.

$$\begin{cases} [\delta_{\mathrm{ex}}^{i} = 1] \leftrightarrow [\omega_{\mathrm{e}} \in A_{\mathrm{e}}^{i}], & i = 1,2,\ldots,3, \\ [\delta_{gx}^{i} = 1] \leftrightarrow [\omega_{\mathrm{g}} \in A_{\mathrm{g}}^{i}], & i = 1,2,\ldots,5, \\ [\delta_{\mathrm{mx}}^{i} = 1] \leftrightarrow [\omega_{\mathrm{m}} \in A_{\mathrm{m}}^{i}], & i = 1,2,\ldots,7. \end{cases} \tag{11}$$

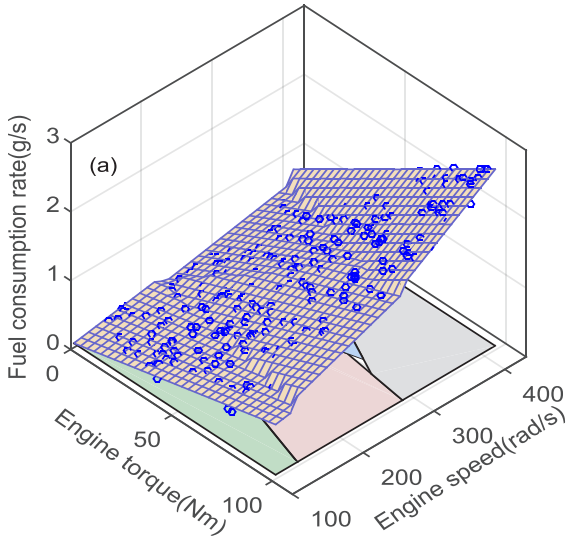

(a) Linearization of engine fuel consumption rate

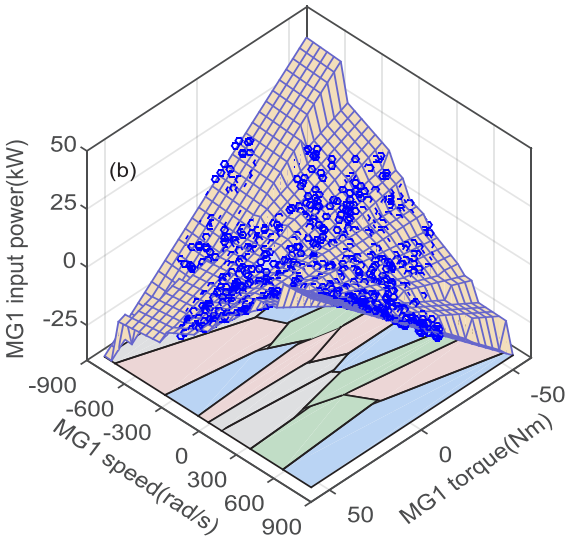

(b) Linearization of the MG1 input power

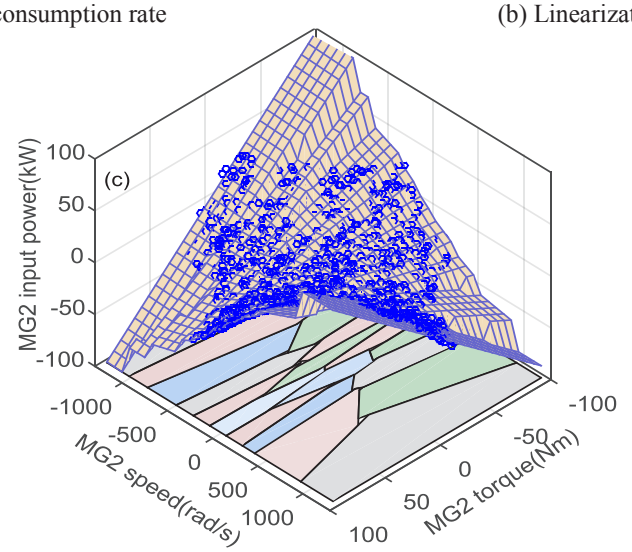

(c) Linearization of the MG2 input power

Fig. 5. Linearization of three-dimensional models

According to the requirement for curve piecewise approximation, auxiliary continuous variables T_{ex}^i, T_{gx}^i and T_{mx}^i are introduced and expressed as follows:

$$\begin{cases} T_{\mathrm{ex}}^i = \{\text{IF } \delta_{\mathrm{ex}}^i \text{ THEN } [\omega_{\mathrm{e}}\ 1]\theta_{\mathrm{ex}}^i \\ \qquad\qquad \text{ELSE } 0\}, \quad i=1,2\ldots,3, \\ T_{\mathrm{gx}}^i = \{\text{IF } \delta_{\mathrm{gx}}^i \text{ THEN } [\omega_{\mathrm{g}}\ 1]\theta_{\mathrm{gx}}^i \\ \qquad\qquad \text{ELSE } 0\}, \quad i=1,2\ldots,5, \\ T_{\mathrm{mx}}^i = \{\text{IF } \delta_{\mathrm{mx}}^i \text{ THEN } [\omega_{\mathrm{m}}\ 1]\theta_{\mathrm{mx}}^i \\ \qquad\qquad \text{ELSE } 0\}, \quad i=1,2\ldots,7. \end{cases} \tag{12}$$

Then, T_{ex}, T_{gx} and T_{mx} can be approximately expressed as follows:

$$\begin{cases} T_{\mathrm{ex}} = T_{\mathrm{ex}}^1 + T_{\mathrm{ex}}^2 + T_{\mathrm{ex}}^3, \\ T_{\mathrm{gx}} = T_{\mathrm{gx}}^1 + T_{\mathrm{gx}}^2 + \ldots + T_{\mathrm{gx}}^5, \\ T_{\mathrm{mx}} = T_{\mathrm{mx}}^1 + T_{\mathrm{mx}}^2 + \ldots + T_{\mathrm{mx}}^7. \end{cases} \tag{13}$$

The energy management strategy of power split HEV focuses on steady power distribution to improve the vehicle fuel economy. It means that the transient start-up and shut-down characteristics of the engine and electric machines can be ignored. Therefore, by ignoring the start-up and shut-down process of different power sources, the engine has two working states, as follows:

$$\begin{cases} \{(T_{\mathrm{e}}, \omega_{\mathrm{e}})|\ T_{\mathrm{e}}=0,\ \ \omega_{\mathrm{e}}=0\}, \\ \{(T_{\mathrm{e}}, \omega_{\mathrm{e}})|\ 0<T_{\mathrm{e}}\le T_{\mathrm{ex}},\ \ \omega_{\mathrm{es}}\le\omega_{\mathrm{e}}\le\omega_{\mathrm{ex}}\}. \end{cases} \tag{14}$$

A reverse operation is not considered in the study. Hence, the vehicle has three states: driving, braking and standstill. The corresponding input sets are:

$$\begin{cases} \{(T_{\mathrm{req}}, \omega_{\mathrm{out}})|\ T_{\mathrm{req}}>0,\ \ \omega_{\mathrm{out}}\ge 0\}, \\ \{(T_{\mathrm{req}}, \omega_{\mathrm{out}})|\ T_{\mathrm{req}}\le 0,\ \ \omega_{\mathrm{out}}>0\}, \\ \{(T_{\mathrm{req}}, \omega_{\mathrm{out}})|\ T_{\mathrm{req}}=0,\ \ \omega_{\mathrm{out}}=0\}. \end{cases} \tag{15}$$

Auxiliary discrete variable δ_{M}^i $(i=1,2,\ldots,6)$ is defined to represent pure electric driving, engine driving, hybrid driving, compound braking, charging standstill and stop mode, respectively. By combining the working state sets of different power sources and the state set of disturbance input (the required torque T_{req} and rotational speed ω_{out}), the equivalent torque and speed constraints corresponding to the discrete variables δ_{M}^i of different modes can be derived, as shown by the following equivalence between the discrete variable and constraint combinations.

$$\begin{cases} [\delta_{\mathrm{M}}^1{=}1] \leftrightarrow [T_{\mathrm{e}}{=}0]\wedge[\omega_{\mathrm{e}}{=}0]\wedge[0<T_{\mathrm{req}}] \\ \quad \wedge[0\le\omega_{\mathrm{out}}]\wedge[\omega_{\mathrm{m}}\le\omega_{\mathrm{mx}}] \\ \quad \wedge[T_{\mathrm{req}}/(1{+}k_2)\le T_{\mathrm{mx}}], \\ [\delta_{\mathrm{M}}^2{=}1] \leftrightarrow [0<T_{\mathrm{e}}\le T_{\mathrm{ex}}]\wedge[\omega_{\mathrm{es}}\le\omega_{\mathrm{e}}\le\omega_{\mathrm{ex}}] \\ \quad \wedge[0<T_{\mathrm{req}}]\wedge[0\le\omega_{\mathrm{out}}] \\ \quad \wedge[\omega_{\mathrm{e}}{=}k_1/(1{+}k_1)\omega_{\mathrm{out}}]\wedge[T_{\mathrm{e}}{=}(1{+}k_1)/k_1 T_{\mathrm{req}}], \\ [\delta_{\mathrm{M}}^3{=}1] \leftrightarrow [0<T_{\mathrm{e}}\le T_{\mathrm{ex}}]\wedge[\omega_{\mathrm{es}}\le\omega_{\mathrm{e}}\le\omega_{\mathrm{ex}}] \\ \quad \wedge[0<T_{\mathrm{req}}]\wedge[0\le\omega_{\mathrm{m}}]\wedge([T_{\mathrm{e}}\ne(1{+}k_1)k_1^{-1}T_{\mathrm{req}}] \\ \quad \vee[\omega_{\mathrm{e}}\ne k_1(1+k_1)^{-1}\omega_{\mathrm{out}}]), \\ \quad \wedge[-\omega_{\mathrm{mx}}\le\omega_{\mathrm{m}}\le\omega_{\mathrm{mx}}]\wedge[-\omega_{gx}\le\omega_{\mathrm{g}}\le\omega_{gx}] \\ \quad \wedge[-T_{\mathrm{mx}}\le[(1{+}k_1)T_{\mathrm{req}}{-}k_1T_{\mathrm{e}}]/(1{+}k_1{+}k_2)\le T_{\mathrm{mx}}] \\ \quad \wedge[-T_{gx}\le[k_2T_{\mathrm{req}}{-}(1{+}k_2)T_{\mathrm{e}}]/(1{+}k_1{+}k_2)\le T_{\mathrm{gx}}], \\ [\delta_{\mathrm{M}}^4{=}1] \leftrightarrow [T_{\mathrm{e}}{=}0]\wedge[\omega_{\mathrm{e}}{=}0]\wedge[T_{\mathrm{req}}\le 0]\wedge[0<\omega_{\mathrm{out}}], \\ [\delta_{\mathrm{M}}^5{=}1] \leftrightarrow [0<T_{\mathrm{e}}\le T_{\mathrm{ex}}]\wedge[\omega_{\mathrm{es}}\le\omega_{\mathrm{e}}\le\omega_{\mathrm{ex}}] \\ \quad \wedge[T_{\mathrm{req}}{=}0]\wedge[\omega_{\mathrm{out}}{=}0]\wedge[\omega_{\mathrm{g}}\le\omega_{\mathrm{gx}}] \\ \quad \wedge[T_{\mathrm{e}}/(1+k_1)\le T_{\mathrm{gx}}], \\ [\delta_{\mathrm{M}}^6{=}1] \leftrightarrow [T_{\mathrm{e}}{=}0]\wedge[\omega_{\mathrm{e}}{=}0]\wedge[T_{\mathrm{req}}=0]\wedge[\omega_{\mathrm{out}}{=}0]. \end{cases} \tag{16}$$

The above formula includes all possible input combinations of the system. The state of the coupling mechanism can be determined by the HEV working mode, and the torque model can also be determined. Before expressing the motor torque, the composite braking situation needs to be processed. Auxiliary discrete variables δ_{s}^1 and δ_{s}^2 are defined to satisfy the following requirements:

$$\begin{cases} [\delta_{\mathrm{s}}^1=1] \leftrightarrow [T_{\mathrm{req}}/(1+k_2)\ge -T_{\mathrm{mx}}], \\ [\delta_{\mathrm{s}}^1=1] \leftrightarrow [\omega_{\mathrm{m}}\ge\omega_{\mathrm{mx}}]. \end{cases} \tag{17}$$

MG1 and MG2 torque is expressed by continuous variables T_g^i $(i=1,2,3)$ and T_m^i $(i=1,2,3,4)$, respectively:

$$\begin{cases} T_{\mathrm{g}}^1 = \{\text{IF } \delta_{\mathrm{M}}^1\vee\delta_{\mathrm{M}}^2\vee\delta_{\mathrm{M}}^4\vee\delta_{\mathrm{M}}^6 \text{ THEN } 0 \text{ ELSE } 0\}, \\ T_{\mathrm{g}}^2 = \{\text{IF } \delta_{\mathrm{M}}^3 \text{ THEN } [k_2T_{\mathrm{req}}{-}(1{+}k_2)T_{\mathrm{e}}]/(1{+}k_1{+}k_2) \\ \qquad\qquad\qquad\qquad \text{ELSE } 0\}, \\ T_{\mathrm{g}}^3 = \{\text{IF } \delta_{\mathrm{M}}^5 \text{ THEN } -T_{\mathrm{e}}/(1+k_1) \text{ ELSE } 0\}; \end{cases} \tag{18}$$

$$\begin{cases} T_{\mathrm{m}}^1 = \{\text{IF } \delta_{\mathrm{M}}^1\vee(\delta_{\mathrm{M}}^4\wedge(\sim\delta_{\mathrm{s}}^2)\wedge\delta_{\mathrm{s}}^1) \\ \qquad \text{THEN } T_{\mathrm{req}}/(1+k_2) \text{ ELSE } 0\}, \\ T_{\mathrm{m}}^2 = \{\text{IF } \delta_{\mathrm{M}}^2\vee\delta_{\mathrm{M}}^5\vee\delta_{\mathrm{M}}^6\vee(\delta_{\mathrm{M}}^4\wedge\delta_{\mathrm{s}}^2) \\ \qquad \text{THEN } 0 \text{ ELSE } 0\}, \\ T_{\mathrm{m}}^3 = \{\text{IF } \delta_{\mathrm{M}}^3 \text{ THEN} \\ \qquad [(1{+}k_1)T_{\mathrm{req}}{-}k_1T_{\mathrm{e}}]/(1{+}k_1{+}k_2) \text{ ELSE } 0\}, \\ T_{\mathrm{m}}^4 = \{\text{IF } \delta_{\mathrm{M}}^4\wedge(\sim\delta_{\mathrm{s}}^2)\wedge(\sim\delta_{\mathrm{s}}^1) \\ \qquad \text{THEN } -T_{\mathrm{mx}} \text{ ELSE } 0\}. \end{cases} \tag{19}$$

Therefore, the torques of MG1 and MG2 are expressed by the following formula:

$$\begin{cases} T_{\mathrm{g}} = T_{\mathrm{g}}^1 + T_{\mathrm{g}}^2 + T_{\mathrm{g}}^3, \\ T_{\mathrm{m}} = T_{\mathrm{m}}^1 + T_{\mathrm{m}}^2 + T_{\mathrm{m}}^3 + T_{\mathrm{m}}^4. \end{cases} \tag{20}$$

When the torques and speeds of different components are known, fuel consumption and motor input power can be calculated according to engine fuel consumption surface and motor input power surface. In order to express the engine fuel consumption and motor input power, auxiliary discrete variables δ_{ef}^i, δ_{gp}^i and δ_{mp}^i are defined, as shown by:

$$\begin{cases} \left[\delta_{\mathrm{ef}}^i = 1\right] \leftrightarrow \left[(T_{\mathrm{e}}, \omega_{\mathrm{e}}) \in \Omega_{\mathrm{ef}}^i\right], & i = 1,2,3, \\ \left[\delta_{\mathrm{gp}}^i = 1\right] \leftrightarrow \left[(T_{\mathrm{g}}, \omega_{\mathrm{g}}) \in \Omega_{\mathrm{gp}}^i\right], & i = 1,2,\ldots,14, \\ \left[\delta_{\mathrm{mp}}^i = 1\right] \leftrightarrow \left[(T_{\mathrm{m}}, \omega_{\mathrm{m}}) \in \Omega_{\mathrm{mp}}^i\right], & i = 1,2,\ldots,18. \end{cases} \tag{21}$$

Further, auxiliary continuous variables f_{e}^i, P_{gp}^i and P_{mp}^i are introduced and expressed as follows:

$$\begin{cases} f_{\mathrm{e}}^i = \{\text{IF } \delta_{\mathrm{ef}}^i \text{ THEN } [T_{\mathrm{e}}\ \omega_{\mathrm{e}}\ 1]\theta_{\mathrm{ef}}^i \\ \qquad\qquad \text{ELSE } 0, \quad i = 1,2,3,4, \\ P_{\mathrm{gp}}^i = \{\text{IF } \delta_{\mathrm{gp}}^i \text{ THEN } [T_{\mathrm{g}}\ \omega_{\mathrm{g}}\ 1]\theta_{\mathrm{gp}}^i \\ \qquad\qquad \text{ELSE } 0, \quad i = 1,2,\ldots,14, \\ P_{\mathrm{mp}}^i = \{\text{IF } \delta_{\mathrm{mp}}^i \text{ THEN } [T_{\mathrm{m}}\ \omega_{\mathrm{m}}\ 1]\theta_{\mathrm{mp}}^i \\ \qquad\qquad \text{ELSE } 0, \quad i = 1,2,\ldots,18. \end{cases} \tag{22}$$

Thus, the engine fuel consumption *fuel* and motor input power P_{gp} and P_{mp} are expressed as:

$$\begin{cases} fuel = f_{\mathrm{e}}^1 + f_{\mathrm{e}}^2 + f_{\mathrm{e}}^3, \\ P_{\mathrm{gp}} = P_{\mathrm{gp}}^1 + P_{\mathrm{gp}}^2 + \ldots + P_{\mathrm{gp}}^{14}, \\ P_{\mathrm{mp}} = P_{\mathrm{mp}}^1 + P_{\mathrm{mp}}^2 + \ldots + P_{\mathrm{mp}}^{18}. \end{cases} \tag{23}$$

In order to improve model accuracy, input power of the motor is processed as follows:

$$\begin{cases} P_{\mathrm{g\_in}} = \{\text{IF } \delta_{\mathrm{M}}^3 \vee \delta_{\mathrm{M}}^5 \text{ THEN } P_{\mathrm{gp}} \text{ ELSE } 0\}, \\ P_{\mathrm{m\_in}} = \{\text{IF } \delta_{\mathrm{M}}^1 \vee \delta_{\mathrm{M}}^3 \vee \delta_{\mathrm{M}}^4 \text{ THEN } P_{\mathrm{mp}} \text{ ELSE } 0\}. \end{cases} \tag{24}$$

where $P_{\mathrm{g\_in}}$ and $P_{\mathrm{m\_in}}$ are modified motor input powers.

Input power of the motor directly determines the SOC change rate. Therefore, auxiliary discrete variable δ_{bs}, which relates to the battery operation state, is defined as:

$$[\delta_{bs} = 1] \leftrightarrow [P_{\mathrm{batt}} \in A_{\mathrm{batt}}^1], \tag{25}$$

where P_{batt} is battery power, which can be expressed as the sum of input power of two motors and $P_{\mathrm{batt}} = P_{\mathrm{g\_in}} + P_{\mathrm{m\_in}}$. Then, the change rate of battery SOC C_{bs} can be described as:

$$C_{\mathrm{bs}} = \{\text{IF } \delta_{\mathrm{bs}} \text{ THEN } [P_{\mathrm{batt}}\ 1]\theta_{\mathrm{bx}}^1 \text{ ELSE } [P_{\mathrm{batt}}\ 1]\theta_{\mathrm{bx}}^2\}. \tag{26}$$

Based on the auxiliary variables, evolution laws of different state variables can be obtained. In this paper, only one continuous state variable, the battery SOC, is selected in the energy management system. The battery SOC model is:

$$\dot{\mathrm{SOC}} = -\frac{V_{\mathrm{oc}} - \sqrt{V_{\mathrm{oc}}^2 - 4P_{\mathrm{batt}}R_{\mathrm{int}}}}{2Q_{\mathrm{bat}}R_{\mathrm{int}}}, \tag{27}$$

where V_{oc} and R_{int} are the battery open-circuit voltage and internal resistance, respectively; and Q_{bat} is the battery capacity. Since the SOC is constrained to a small region, these parameters can be viewed as constant. As shown by Eq. (26) and Fig. 4(d), the SOC change rate is described by C_{bs} to model battery dynamics with piecewise affine processing of the nonlinear SOC model. Therefore, the evolution law of SOC in discrete form can be expressed as follows:

$$\frac{\mathrm{SOC}(t+1) - \mathrm{SOC}(t)}{\Delta T} = \Delta T C_{\mathrm{bs}}. \tag{28}$$

where ΔT is the sampling time, and it is set to be 1 s.

The HEV must run in one of the operation modes at any time. In order to ensure that the optimization problem has a feasible solution, corresponding logical constraints need to be set up, i.e.:

$$\delta_{\mathrm{M}}^1 + \delta_{\mathrm{M}}^2 + \delta_{\mathrm{M}}^3 + \delta_{\mathrm{M}}^4 + \delta_{\mathrm{M}}^5 + \delta_{\mathrm{M}}^6 = 1. \tag{29}$$

According to the above process, the MLD model for the energy management system of the proposed power split HEV can be directly compiled by means of HYSDEL software to obtain a standard mathematical form. The compiled model consists of four input variables, one output variable, one state variable and 633 mixed integer linear inequality constraints. All variables of the compiled model need to be satisfied.

$$\begin{cases} \boldsymbol{x}(t+1) = \boldsymbol{x}(t) + \boldsymbol{B}_3 z(t), \\ \boldsymbol{y}(t) = \boldsymbol{D}_3 z(t), \\ \boldsymbol{E}_2\boldsymbol{\delta}(t) + \boldsymbol{E}_3 z(t) \le \boldsymbol{E}_1\boldsymbol{u}(t) + \boldsymbol{E}_5, \end{cases} \tag{30}$$

where $\boldsymbol{x}$ is the state variable, $\boldsymbol{x} = [\mathrm{SOC}]$; y is an output variable, $\boldsymbol{y} = [fuel]$; u is the vector for input variables, $\boldsymbol{u} = [T_{\mathrm{req}}\ \ \omega_{\mathrm{out}}\ \ T_{\mathrm{e}}\ \ \omega_{\mathrm{out}}]^T$; z and $\boldsymbol{\delta}$ are all auxiliary continuous variables and discrete variables defined in the modeling process; $\boldsymbol{B}_3$, $\boldsymbol{D}_3$, $\boldsymbol{E}_1$, $\boldsymbol{E}_2$, $\boldsymbol{E}_3$ and $\boldsymbol{E}_5$ are coefficient matrices, the values of these matrices are closely related to the auxiliary discrete and continuous variables as well as to the inequalities. Since the dimensions of these matrices are very large, detailed values are not presented in the manuscript for simplification. Compared with Eq. (7), zero matrices $\boldsymbol{B}_1$, $\boldsymbol{B}_2$, $\boldsymbol{C}$, $\boldsymbol{D}_1$, $\boldsymbol{D}_2$ and $\boldsymbol{E}_4$ in the above equation are eliminated. There are a lot of heuristic propositions hidden in the above modeling process. Addition of these propositions can greatly speed up solution of the controller.

4. Hybrid model predictive control

4.1. Control structure of the HEV. Figure 6 presents the closed loop control diagram of the HEV. The difference between target velocity and actual velocity is sent to the driver

module, which simulates driver operation to calculate the required driving torque that ensures vehicle velocity tracking. The driver model is simulated by a PI controller. The hierarchical control scheme is adopted in the energy management strategy. The required torque derived from driver module is sent to the supervisory controller, where hybrid model predictive control (HMPC) is applied. The optimal engine operation point and vehicle operation mode is firstly calculated in the supervisory controller. Then, based on this information, detailed control variables such as MG1 torque, MG2 torque, operation states of brakes 1 and 2 are further obtained and put on the powertrain by the bottom controller. The output of the powertrain works as feedback for the driver and controller.

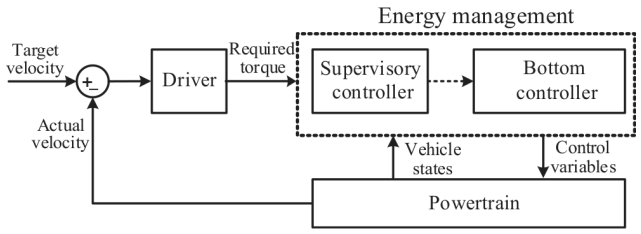

Fig. 6. Closed loop control of HEV

4.2. Establishment of HMPC. Similarly to conventional MPC, HMPC obtains the optimal control sequence by solving a finite time horizon optimization problem at each sampling time. Only the first element of the control sequence is applied to the powertrain. With iterative repeat, receding optimization is realized [26,27]. Uniquely, with the MLD model being the control-oriented predictive model in HMPC, the optimal solution process requires dealing with continuous and binary variables.

Bearing in mind that fuel economy of the HEV depends on the engine fuel consumption and the usage of electrical energy, the assessment of usage of electrical energy should be conducted by variation of the battery SOC, where the differences between the actual SOC value and the reference value are compared. Therefore, the performance index is set as:

$$L=\int_{t}^{t+\Delta t}\left(q_{\mathrm{SOC}}\cdot(\mathrm{SOC}(\tau)-\mathrm{SOC}_{\mathrm{ref}})^2+q_{\mathrm{fuel}}\cdot fuel(\tau)^2\right)\mathrm{d}\tau, \quad (31)$$

where t is the sampling time; Δt is the prediction horizon; q_{SOC} and q_{fuel} are corresponding weight factors; and $\mathrm{SOC}_{\mathrm{ref}}$ is the reference SOC.

With the MLD model, the optimal control problem is established as:

$$\begin{aligned}\min J=&\boldsymbol{Q}_{\rho}\rho^2+\sum_{i=1}^{N}\|\boldsymbol{x}(t+i+1)-\boldsymbol{x}_{\mathrm{ref}}\|^2_{\boldsymbol{Q}_x}\\&+\sum_{i=0}^{N-1}\|\boldsymbol{y}(t+i)-\boldsymbol{y}_{\mathrm{ref}}\|^2_{\boldsymbol{Q}_y}\\ subj.\ to\ &\begin{cases}\boldsymbol{x}_0=\boldsymbol{x}(t),\\ \boldsymbol{x}(t+1)=\boldsymbol{x}(t)+\boldsymbol{B}_3\boldsymbol{z}(t),\\ \boldsymbol{y}(t)=\boldsymbol{D}_3\boldsymbol{z}(t),\\ \boldsymbol{E}_2\boldsymbol{\delta}(t)+\boldsymbol{E}_3\boldsymbol{z}(t)\le\boldsymbol{E}_{11}\boldsymbol{u}(t)+\boldsymbol{E}_{12}\boldsymbol{v}(t)+\boldsymbol{E}_5,\end{cases}\end{aligned} \quad (32)$$

where N is the prediction horizon which is set to be the same as the control horizon; $\boldsymbol{x}(t)$ is the state of the MLD system at sampling time t; $\boldsymbol{x}(t+i)$ and $\boldsymbol{y}(t+i)$ are the predicted state vector and output vector, which are determined by the control sequence $\boldsymbol{u}N-1\ 0$, $\boldsymbol{u}N-1\ 0=\{u(0),\ u(1),\ldots,u(N-1)\}$; and $u(t+i)$ is the manipulated variables vector. P is the softening variable used to avoid infeasibility of the optimization problem; $\boldsymbol{Q}_{\boldsymbol{\rho}}$ is its weighting factor. Y_{ref}, ξ_{ref} are reference vectors; $\boldsymbol{Q}_y$ and $\boldsymbol{Q}_x$ are weighting factor vectors for $\boldsymbol{x}$ and $\boldsymbol{y}$; $\boldsymbol{E}_{11}$ and $\boldsymbol{E}_{12}$ are the last two and the first two terms of the $\boldsymbol{E}_1$.

The optimization vector γ, which includes binary and continuous parts, is defined as follows:

$$\begin{aligned}&\gamma\triangleq\begin{bmatrix}\Im\\ \Re\\ \aleph\\ \rho\end{bmatrix},\qquad \Im\triangleq\begin{bmatrix}u(0)\\ \vdots\\ u(N-1)\end{bmatrix},\\ &\Re\triangleq\begin{bmatrix}\delta(0)\\ \vdots\\ \delta(N-1)\end{bmatrix},\qquad \aleph\triangleq\begin{bmatrix}z(0)\\ \vdots\\ z(N-1)\end{bmatrix}.\end{aligned} \quad (33)$$

By combining Eq. (31) and Eq. (32), the optimization problem can be finally transformed into a mixed integer quadratic program (MIQP), where a quadratic cost function is subject to linear constraints [28], as shown in Eq. (34):

$$\begin{aligned}&\min_{\gamma}\left(\frac{1}{2}\gamma^T H\gamma+F\gamma\right),\\ &s.t.\quad\begin{cases}A_{ineq}\gamma\le b_{ineq},\\ A_{eq}\gamma=b_{eq},\\ lb\le\gamma\le lu,\\ \gamma\in R^{nc}\times\{0,1\}^{nd}\end{cases}\end{aligned} \quad (34)$$

where $\boldsymbol{H}$, $\boldsymbol{F}$, $\boldsymbol{A}_{\mathrm{ineq}}$, $\boldsymbol{A}_{\mathrm{eq}}$, $\boldsymbol{b}_{\mathrm{ineq}}$, $\boldsymbol{b}_{\mathrm{eq}}$, $\boldsymbol{lb}$, $\boldsymbol{lu}$ are the coefficient matrices. γ is the optimization vector, including binary and continuous parts.

Although the MIQP problem has exponential complexity with the combination of continuity and binary variables, the application of efficient numerical tools can solve the optimization quickly [29].

5. Simulation and analysis

Forward simulations under the Urban Dynamometer Driving Schedule (UDDS), Highway Fuel Economy Test (HWFET) and Worldwide harmonized Light duty Test Cycle (WLTC) are conducted to evaluate controller performance [30]. Table 2 lists the vehicle parameters. Specifications of the HEV are referred to those of the Toyota Prius. Parameters are detailed in the ADVISOR software. In order to ensure enough margin of the battery for charging and discharging, the initial battery SOC is set at 0.55. The simulation step is set to be 1 second. In terms

Table 2
Specifications of HEV

Parameter	Value
Coefficient of rolling resistance f	0.008
Wheel radius r	0.287 m
Vehicle frontal area A	1.746 m^2
Air drag coefficient C_d	0.3
Air density ρ	1.23
Characteristic parameters k_1/k_2	1.842/2.48
Final drive ratio i_d	3.93
Engine inertia I_e	0.072 kg · m^2
Engine maximum speed $\omega_{e\max}$	4700 rpm
Engine maximum power $P_{e\max}$	54 kw
MG1 inertia I_{MG1}	0.022 kg · m^2
MG1 maximum speed $\omega_{MG1\max}$	8000 rpm
MG1 maximum power $P_{e\max}$	15 kw
MG2 inertia I_{MG2}	0.030 kg · m^2
MG2 maximum speed $\omega_{MG2\max}$	15000 rpm
MG2 maximum power $P_{e\max}$	30 kw
k_1, k_2	2.11/2.11

of fuel economy evaluation, such step is acceptable. With the increase of the prediction horizon, more future information can be applied, but it will also result in an increase of computational complexity. Therefore, for real-time application, prediction horizon N is set to be 2 to reduce the computational burden.

Since the control goal is to ensure minimal engine fuel consumption and maintain battery charging sustainability, the reference values of engine fuel consumption $fuel_{ref}$ and battery SOC SOC_{ref} are set at 0 and 0.55, respectively. By setting the weighting factor of engine fuel consumption q_{fuel} at 1, only the weighting factor q_{SOC} needs to be adjusted. When q_{SOC} is very large, the battery SOC is more likely to fluctuate along the reference value, and the differences between the actual SOC and the reference value are always small, thereby constraining the final SOC effectively. However, the battery power regulating performance cannot be fully utilized, resulting in poor performance of the HEV. When q_{SOC} is very small, final battery SOC can easily deviate from the reference value to a large extent. The decision of q_{SOC} should ensure good battery charging sustainability and power regulating performance. By means of such expert knowledge and iterative parameter calibration, the weighting factor q_{SOC} is set at 15000.

Figure 7 details the engine fuel map, in which the engine fuel consumption (with the unit as g/kWh) is decided by engine speed and torque. The maximal torque and optimal operation line (OOL) are also depicted in Fig. 7, where the former constrains the engine output torque and the latter ensures high operation efficiency of the engine. The OOL is decided according to the optimal engine speed and torque for different power levels, which has been detailed in Ref. [6]. The OOL ensures the minimum engine fuel consumption for different power levels. In order to evaluate the control effect of the proposed strategy, the rule based control strategy based on the engine OOL is also established. The engine operations points are controlled to be located along the OOL. Due to good robustness and superior real-time performance, the OOL control strategy has been used widely and demonstrates effective performance in reducing fuel consumption [31].

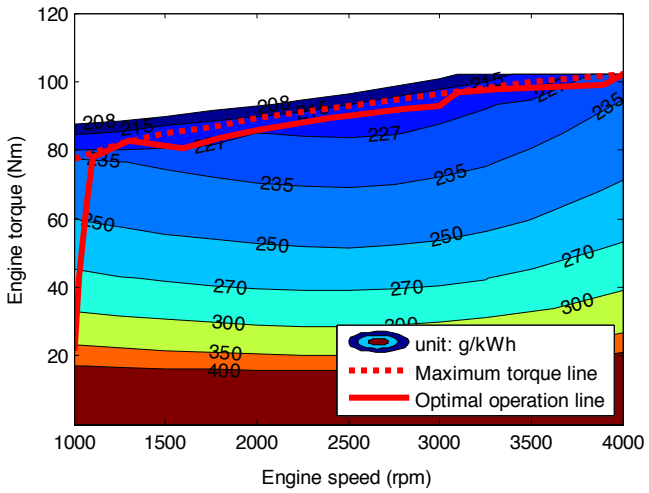

Fig. 7. Engine fuel map

Figures 8–10 show the response curves of different power components under the three different running conditions. For simplification, rule based control strategy and hybrid model predictive control strategy are abbreviated as rule based and optimization based, respectively.

Figures 8a–10a give the velocity profiles under different driving cycles as well as the velocity tracking performance for different cycles. It is obvious that the actual vehicle speed is very close to the target vehicle speed with the two strategies, which shows that both control strategies can effectively maintain the driving state of the vehicle. The ideal velocity tracking performance is the premise to accurately evaluate the fuel economy of the vehicle, which also verifies the correctness of the vehicle model.

From Fig. 8–10, it is seen that the power of different components fluctuates within their allowable range under all the test driving conditions. Compared with the simulation results under HWFET and WLTC, the instantaneous on/off characteristics of the engine under UDDS are more significant. It is because frequent instantaneous acceleration and deceleration under UDDS results in higher output frequency of the engine, thus the power curve is relatively more intensive. It can be seen from Fig. 8b that although the engine with optimization based control strategy runs longer than that with rule based strategy, i.e. the engine operating times are 573 s and 453 s, respectively, the average power of optimization based control is lower. The average power of the engine is 5.71 kW and 8.59 kW for opti-

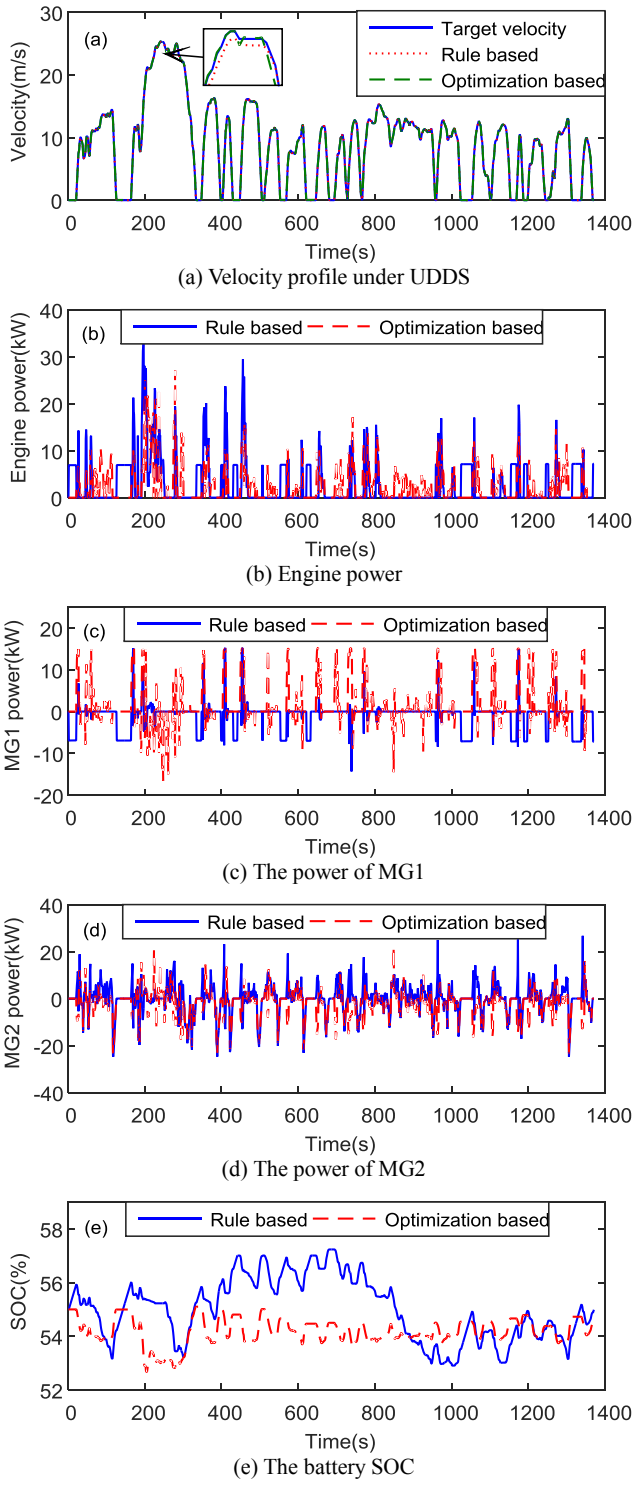

(a) Velocity profile under UDDS
(b) Engine power
(c) The power of MG1
(d) The power of MG2
(e) The battery SOC

Fig. 8. Simulation results under UDDS

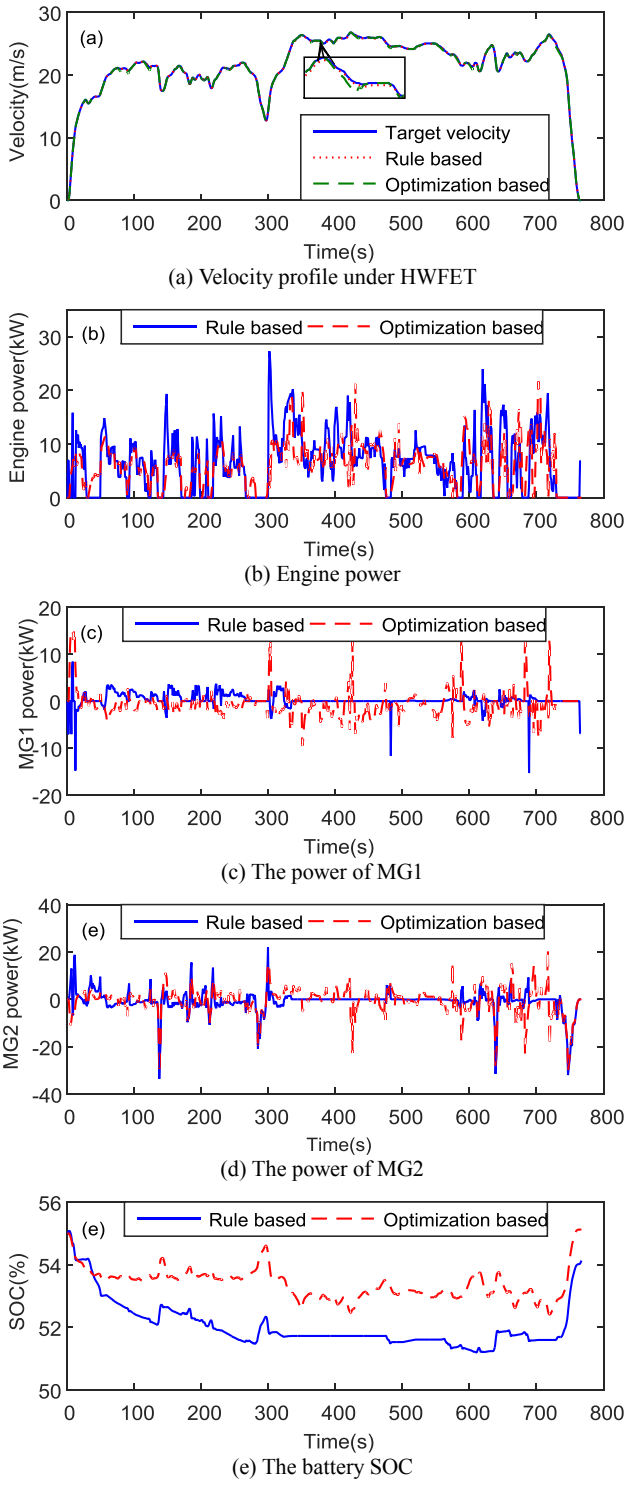

(a) Velocity profile under HWFET
(b) Engine power
(c) The power of MG1
(d) The power of MG2
(e) The battery SOC

Fig. 9. Simulation results under HWFET

mization and rule based strategies, respectively. Consequently, the overall fuel consumption of the engine with optimization based strategy is still at a low level.

As shown by Fig. 8c and Fig. 8d, the power of MG1 and MG2 fluctuates positively and negatively to regulate the engine operation points according to the driving condition of the vehicle. When the ratio of the engine speed to output shaft speed is between the two mechanical points, the power of MG1 is negative. Otherwise, the power of MG1 is positive. During the braking process, MG2 provides negative torque to regenerate braking energy. Fig. 8e shows that under the two control strategies, the battery SOC is maintained at a reasonable level. Because deviation between the actual battery SOC and reference value is added in the objective function for optimal

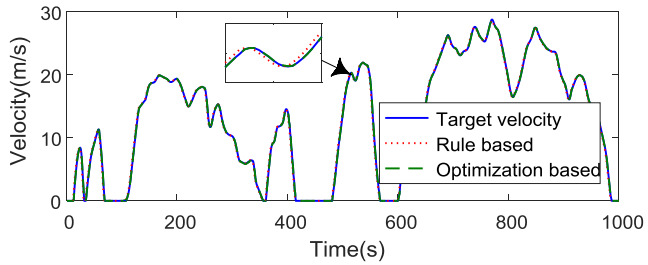

(a) Velocity profile under WLTC

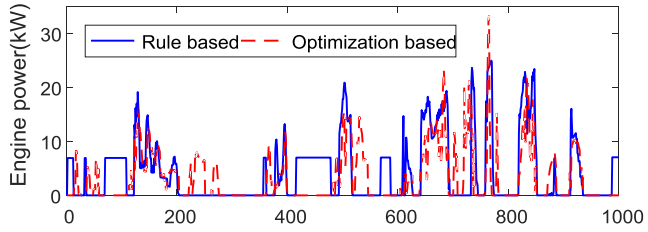

(b) Engine power

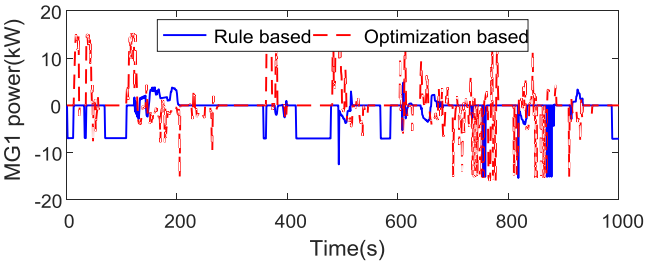

(c) The power of MG1

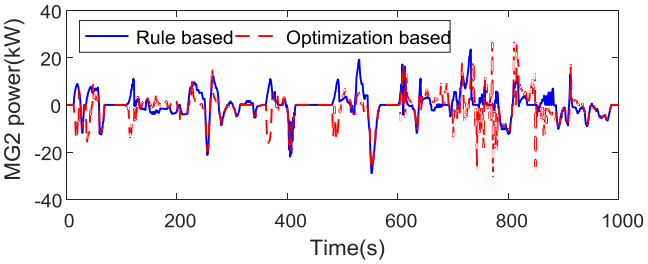

(d) The power of MG2

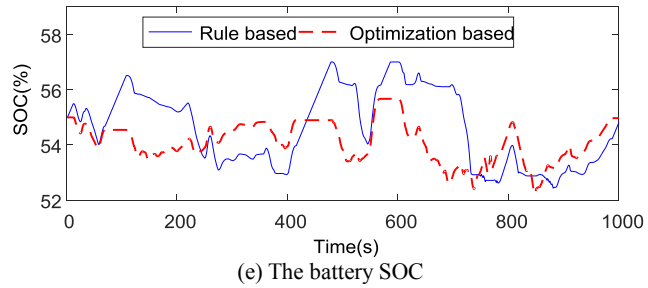

(e) The battery SOC

Fig. 10. Simulation results under WLTC

control, the battery SOC is effectively maintained to remain at around 0.55.

Under HWFET, vehicle velocity is very high while velocity change is relatively smooth. According to Fig. 9a–9d, the vehicle with rule based strategy mainly works in engine driving mode for the high-speed operation regions between 330 s and 580 s according to the control logic. In this case, all the power comes from the engine, and the powers of MG1 and MG2 are zero. And the battery SOC remains unchanged. However, when the optimization based strategy is applied, the vehicle operates in the hybrid driving mode for these high-speed regions, and all the power components are involved in the driving. It can be seen that the mode switching rules formulated by human experience have greater subjectivity and limitations, thus optimal fuel economy of the vehicle in practical applications cannot be guaranteed.

Under WLTC, it can be seen that the vehicle with rule based strategy operates in charging standstill mode when velocity is zero. In this way, MG1 is driven by the engine to charge the battery so as to maintain battery charging sustainability. When the optimization based strategy is applied, the on/off states of MG1 in the time region between 740 s and 755 s change frequently, as shown by Fig. 10c. Besides, it is seen that there is more positive output power of MG1 with the proposed optimization based strategy. According to Fig. 10e, the battery SOC with HMPC is nearly exactly maintained by constraining the SOC variation.

Due to the difference of the final battery SOC, the actual engine fuel consumption alone is not enough to evaluate the fuel economy. The evaluation must cover both the engine fuel consumption and the usage of electrical energy. Therefore, the deviation between the initial SOC and the final SOC is converted into equivalent fuel consumption of the engine. Then equivalent fuel consumption is introduced.

Table 3 lists the fuel economy of the power split HEV, where "FC" represents engine fuel consumption, "EFC" represents equivalent fuel consumption, which contains equivalent fuel consumption of electrical energy, "ΔSOC" represents the change of battery SOC and "↑EFC" represents the improvement in equivalent fuel economy. The results show that, compared with rule based control, optimization based control has more obvious advantages in energy saving. Under WLTC, as compared with the optimal strategy based on the proposed HMPC, the rule based strategy using OOL shows larger battery discharging and higher engine fuel consumption (FC). The advantage of the proposed strategy is highlighted. Equivalent fuel economy under different test conditions is improved to different degrees. Equivalent fuel consumption of the vehicle under UDDS, HWFET and WLTC is reduced by 7.6%, 8.4% and 5.1%, respectively.

Table 3
Fuel economy of power split HEV

Running cycles	Control strategies	FC (L/100 km)	ΔSOC (%)	EFC (L/100 km)	↑EFC (%)
UDDS	HMPC	2.717	−0.54	2.771	7.6
	OOL	2.993	−0.05	2.998	
HWFET	HMPC	2.823	0.12	2.811	8.4
	OOL	3.015	−0.83	3.070	
WLTC	HMPC	2.761	−0.05	2.766	5.1
	OOL	2.892	−0.25	2.916	

6. Conclusion

The power split HEV with two brakes integrated in the planetary gear sets are proposed in the paper. The operation characteristic of the proposed HEV is analyzed, and found to be featuring interactions between continuous state evolution and discrete mode switches during the energy management process. In order to deal with the energy management problem of this kind of HEVs, a novel control strategy, HMPC, is proposed, based on the hybrid system theory. The MLD modeling method is applied to establish the unified control-oriented model and accurately describe the hybrid nature of the energy management system. By introducing binary variables, the switching behavior between different operation modes is described and modeled together with the continuous process of the power distribution. To facilitate establishment of the MLD model for the power split HEV, piecewise affine technology is adopted to linearize the nonlinear components. On this basis, HMPC is used to derive the optimal control sequence, where the optimization problem is transformed into a mixed integer quadratic program with the engine fuel consumption and the variation of the battery SOC as objective function. Simulation studies under different scenarios show that the proposed control strategy has superior fuel economy as compared with the widely applied rule based strategy. Improvements in terms of equivalent fuel economy are about 7.6%, 8.4% and 5.1% for the UDDS, HWFET and WLTC scenarios, respectively.

Acknowledgements. This work is funded by the National Natural Science Foundation of China (Grant No. 51905219, 51475213 and U1764257), the Natural Science Foundation of Jiangsu Province (Grant No. BK20190844 and BK20180100), the Postdoctoral Science Foundation of China (Grant No. 2019M661752), the Natural Science Research Project of Jiangsu Higher Education Institutions (Grant No. 19KJB580001), the Foundation for Vehicle Measurement, the Control and Safety Key Laboratory of Sichuan Province (QCCK2020-004), the Key Research and Development Program of Zhenjiang City (GY2020020), and the National Key Research and Development Program of China (2018YFB0105003).

References

[1] J.J. Hu, B. Mei, H. Peng, and X.Y. Jiang, "Optimization design and analysis for a single motor hybrid powertrain configuration with dual planetary gears", *Appl. Sci.* 9(4), 707 (2019).

[2] S.H. Wang, S. Zhang, D.H. Shi, X.Q. Sun, and J.Q. He, "Research on instantaneous optimal control of the hybrid electric vehicle with planetary gear sets", *J. Braz. Soc. Mech. Sci. Eng.* 41(1), 51 (2019).

[3] J. Kim, J. Kang, Y. Kim, T. Kim, B. Min, and H. Kim, "Design of power split transmission: design of dual mode power split transmission", *Int. J. Automot. Technol.* 11(4), 565–571 (2010).

[4] F. Wang, J. Zhang, X. Xu, Y.F. Cai, Z.G. Zhou, and X.Q. Sun, "New method for power allocation of multi-power sources considering speed-up transient vibration of planetary power-split HEVs driveline system", *Mech. Syst. Sig. Process.* 128, 1–18 (2019).

[5] J.M. Miller, "Hybrid electric vehicle propulsion system architectures of the E-CVT type", *IEEE Trans. Power Electron.* 21(3), 756–767 (2006).

[6] D.H. Shi, S.H. Wang, P. Pisu, L. Chen, R.C. Wang, and R.G. Wang, "Modeling and optimal energy management of a power split hybrid electric vehicle", *Sci. China Technol. Sci.* 60(5), 1–13 (2017).

[7] J.D. Wishart, L. Zhou, and Z. Dong, "Review, modelling and simulation of two-mode hybrid vehicle architecture", *Proceedings of the ASME 2007 International Design Engineering Technical Conferences and Computers and Information in Engineering Conference,* Nevada, USA, 2007, pp. 1091–1112.

[8] L. Chen, F.T. Zhu, M.M. Zhang, Y. Huo, C.L. Yin, and H. Peng, "Design and analysis of an electrical variable transmission for a series–parallel hybrid electric vehicle", *IEEE Trans. Veh. Technol.* 60(5), 2354–2363 (2011).

[9] P. Aishwarya and O.B. Hari, "A review of optimal energy management strategies for hybrid electric vehicle", *Int. J. Veh. Tech.* 160510 (2014).

[10] B.L.C. Cezar and O. Alexandru, "A dynamic programming control strategy for HEV", *Appl. Mech. Mater.* 263, 541–544 (2013).

[11] J. Park, "Development of equivalent fuel consumption minimization strategy for hybrid electric vehicles", *Int. J. Automot. Technol.* 13(5), 835–843 (2012).

[12] D.H. Shi, P. Pisu, and L. Chen, "Control design and fuel economy investigation of power split HEV with energy regeneration of suspension", *Appl. Energy.* 182, 576–589 (2016).

[13] T. Tarczewski, M. Skiwski, L.J. Niewiara, and L.M. Grzesiak, "High-performance PMSM servo-drive with constrained state feedback position controller", *Bull. Pol. Acad. Sci. Tech. Sci.* 66(1), 49–58 (2018).

[14] H. Borhan, A. Vahidi, A.M. Phillips, M.L. Kuang, I.V. Kolmanovsky, and S.D. Cairano, "MPC-based energy management of a power-split hybrid electric vehicle", *IEEE Trans. Control Syst. Technol.* 20(3), 593–603 (2012).

[15] A. Babiarz, A. Czornik, J. Klamka, and M. Niezabitowski, "The selected problems of controllability of discrete-time switched linear systems with constrained switching rule", *Bull. Pol. Acad. Sci. Tech. Sci.* 63(3), 657–666 (2015).

[6] S.G. Olsen and G.M. Bone, "Model-based control of three degrees of freedom robotic bulldozing", *J. Dyn. Syst. Meas. Control.* 136(136), 729–736 (2014).

[17] X.Q. Sun, Y.F. Cai, S.H. Wang, X. Xu, and L. Chen, "Optimal control of intelligent vehicle longitudinal dynamics via hybrid model predictive control", *Rob. Auton. Syst.* 112, 190–200 (2019).

[18] S.G. Olsen and G.M. Bone, "Development of a hybrid dynamic model and experimental identification of robotic bulldozing", *J. Dyn. Syst. Meas. Control.* 135(2), 450–472 (2013).

[19] F.T. Zhu, L. Chen, and C.L. Yin, "Design and analysis of a novel multimode transmission for a hev using a single electric machine", *IEEE Trans. Veh. Technol.* 62(3), 1097–1110 (2013).

[20] R.J. Zhang and Y.B. Chen, "Control of hybrid dynamical systems for electric vehicles", *Proceedings of the 2001 American Control Conference. (Cat. No.01CH37148),* Arlington, VA, USA, 2001, pp. 2884–2889.

[21] J. Lygeros, S. Sastry, and C. Tomlin, *Hybrid Systems: foundations, advanced topics and applications*, University of California, Berkeley, 2012.

[22] X.Q. Sun, Y.F. Cai, S.H. Wang, X.Xu, and L. Chen, "Piecewise affine identification of tire longitudinal properties for autonomous driving control based on data-driven", *IEEE Access* 6, 47424–47432 (2018).

[23] A. Bemporad, A. Garulli, S. Paoletti, and A. Vicino, "A bounded-error approach to piecewise affine system identification", *IEEE Trans. Autom. Control.* 50(10), 1567–1580 (2005).

[24] G. Ferrari-Trecate, M. Muselli, and D. Liberati, "A clustering technique for the identification of piecewise affine systems", *Automatica*. 39(2), 205–217 (2003).

[25] F.D. Torrisi and A. Bemporad, "Hysdel-a tool for generating computational hybrid models for analysis and synthesis problems", *IEEE Trans. Control Syst. Technol.* 12(2), 235–249 (2004).

[26] M. Abdullah and M. Idres, "Constrained model predictive control of proton exchange membrane fuel cell", *J. Mech. Sci. Technol.* 28(9), 3855–3862 (2014).

[27] D. Jolevski and O. Bego, "Model predictive control of gantry/bridge crane with anti-sway algorithm", *J. Mech. Sci. Technol.* 29(2), 827–834 (2015).

[28] G. Ripaccioli, A. Bemporad, F. Assadian, C. Dextreit, S.D. Cairano, and I.V. Kolmanovsky, "Hybrid modeling, identification, and predictive control: An application to hybrid electric vehicle energy management*", International conference on hybrid systems computation and control(HSCC)*, San Francisco, CA, USA, 2009, pp. 321–335.

[29] A. Bemporad and D. Mignone, "Miqp.m: a matlab function for solving mixed integer quadratic programs version 1.02 user guide", ETH–Swiss Federal Institute of Technology, ETHZ–ETL, (2000).

[30] M. Tutuianu *et al.*, "Development of the World-wide harmonized Light duty Test Cycle (WLTC) and a possible pathway for its introduction in the European legislation", *Transp. Res. Part D Transp. Environ.* 40, 61–75 (2015).

[31] N. Kim, S.W. Cha, and H. Peng, "Optimal equivalent fuel consumption for hybrid electric vehicles", *IEEE Trans. Control Syst. Technol.* 20(3), 817–825 (2011).